

Impedance spectroscopy, ionic conductivity and dielectric studies of new Li⁺ ion conducting polymer blend electrolytes based on biodegradable polymers for solid state battery applications

Kalim Deshmukh¹ · M. Basheer Ahamed¹ · Anji Reddy Polu² ·
Kishor Kumar Sadasivuni³ · S. K. Khadheer Pasha⁴ · Deepalekshmi Ponnamma⁵ ·
Mariam Al-Ali AlMaadeed⁵ · Rajendra R. Deshmukh⁶ · K. Chidambaram⁴

Received: 3 May 2016 / Accepted: 28 June 2016 / Published online: 4 July 2016
© Springer Science+Business Media New York 2016

Abstract New solid polymer blend electrolyte films based on biodegradable polymer blend comprising of polyvinyl alcohol (PVA) and poly (*N*-vinyl pyrrolidone) (PVP) doped with different wt% of lithium carbonate (Li₂CO₃) salt have been prepared by solution casting method. The resulting PVA/PVP/Li₂CO₃ polymer blend electrolyte films have been characterized by various analytical techniques such as FTIR, UV–vis, XRD, TGA, polarized optical microscopy and scanning electron microscopy. The FTIR and XRD analysis confirmed the complex formation between PVA/PVP blend and Li₂CO₃ salt. The ionic conductivity and the dielectric properties of PVA/PVP/Li₂CO₃ polymer blend electrolyte films were investigated using an impedance spectroscopy. It was observed that the ionic conductivity of PVA/PVP/Li₂CO₃ electrolyte system increases as a function of Li₂CO₃ concentration. The highest ionic conductivity was found to be $1.15 \times 10^{-5} \text{ S cm}^{-1}$ for polymer blend electrolyte with 20 wt% Li₂CO₃ content. On the

other hand, the dielectric results revealed the non-Debye type of behaviour. The dielectric constant values indicate a strong dielectric dispersion in the studied frequency range which increases as the Li₂CO₃ content increases. The dielectric constant as high as 1200 ($\epsilon = 1201.57$, 50 Hz, 150 °C) and the dielectric loss well below 4 ($\tan \delta = 3.94$, 50 Hz, 150 °C) were obtained for polymer blend electrolytes with 25 wt% Li₂CO₃ salt. Thus, the results obtained in the present study suggest that the PVA/PVP/Li₂CO₃ polymer blend electrolyte system seems to be a promising candidate for solid state battery applications.

1 Introduction

Solid polymer electrolytes have received scientific and technological importance in the last few decades because of their potential applications in various fields such as electrochromic displays, fuel cells, solar cells, sensors, supercapacitors and most importantly rechargeable solid state lithium batteries [1–4]. Lithium batteries have attracted a great deal of attention because of their high energy density, good processability and improved safety [5, 6]. The batteries comprising of solid polymer electrolytes have proven to be cost effective, safe under harsh conditions, environmentally acceptable, provides limitless design flexibility and high performance [7, 8]. It is well known that solid polymer electrolytes have several advantages such as light weight, easy fabrication of thin films of desired shape and size, elimination of leakage current, good mechanical strength, excellent physical and chemical stability and tremendous flexibility in design over their liquid counterparts [9]. However, there are few technical problems with solid polymer electrolytes which include low ambient temperature conductivity, cationic

✉ Kalim Deshmukh
deshmukh.kalim@gmail.com

¹ Department of Physics, B.S. Abdur Rahman University, Chennai, TN 600048, India

² Department of Physics, Vardhaman College of Engineering, Kacharam, Shamshabad, Hyderabad, Telangana 501218, India

³ Mechanical and Industrial Engineering Department, Qatar University, P.O. Box 2713, Doha, Qatar

⁴ Department of Physics, School of Advanced Sciences, VIT University, Vellore, TN 632014, India

⁵ Center for Advanced Materials, Qatar University, P.O. Box 2713, Doha, Qatar

⁶ Department of Physics, Institute of Chemical Technology, Matunga, Mumbai 400019, India

transport number, inadequate thermal stability and poor electrochemical performance of lithium cells below ambient temperature [10, 11]. One of the most important properties of the high-performance solid polymer electrolyte system is their ionic conductivity which depends on the dissociation of ionic conductor and the structure of the polymer matrix [12]. Therefore, the main objective of the research on the solid polymer electrolytes is to enhance their ambient temperature ionic conductivity, mechanical and thermal stability [13]. This is because the solid polymer electrolytes with good ionic conductivity at ambient temperature and excellent mechanical flexibility are very promising candidates for lithium-ion batteries [10]. The ionic conductivity of polymer electrolytes has been attributed to amorphous phases and the interlinking of polymer chains. One of the methods to obtain amorphous phase is by dissolving inorganic acids or lithium salts into suitable polymer matrix using common solvent [14].

Polymer blending is an economical and alternative method for obtaining solid polymer blend electrolyte with optimized physical properties for a wide range of applications [15, 16]. In recent years, blends of polyvinyl alcohol (PVA) and polyvinyl pyrrolidone (PVP) [17], PVA/Chitosan (CN) [18] and PVA/polyethylene glycol (PEG) [15] have been studied by various researchers for the preparation of lithium ion conducting blend polymer electrolytes using various lithium salts such as LiPF_6 , LiCF_3SO_3 , LiClO_4 and LiBF_4 . These studies revealed that the blend polymer electrolyte with different lithium salts exhibit desirable conductivity but poor mechanical and electrochemical stability. In addition to the blending of polymers several other techniques such as cross-linking, the addition of ceramic fillers, block copolymers and plasticizers into the polymer matrix have been employed to enhance the ionic conductivity of solid polymer electrolytes [19]. Among them, polymer blending is very useful and convenient method to develop new materials with desirable electrical conductivity and mechanical stability [20]. The main advantages of polymer blend systems are the easy preparations and the control of physical properties which depends on their miscibility and can be achieved simply by changing the blend compositions [21, 22].

Polyvinyl alcohol (PVA) is one of the most important synthetic polymers because of its low cost, high dielectric strength, good charge storage capacity and dopant dependent physical properties [23, 24]. PVA is non-toxic, biocompatible polymer having good transparency and fast charge transfer at the electrode–electrolyte interface. PVA has been chosen as one of the host polymers for the present study because of its excellent hydrophilic properties, high mechanical strength, good resistance to various chemicals and excellent film forming ability [25, 26].

Several reports are available on organic/inorganic salts complexes with PVA to enhance the ionic conductivity [27, 28] and various PVA-based polymer electrolytes have been reported for electrochemical cell applications [29, 30]. However, PVA-based solid polymer electrolytes exhibit relatively low ionic conductivity. Hence, blending of PVA with other polymers can be a promising and feasible approach to improve ionic conductivity of PVA-based solid polymer electrolytes. Keeping this in mind, polyvinyl pyrrolidone (PVP) was chosen as a second polymer for blending with PVA. PVP is an amorphous polymer which exhibits high glass transition temperature (T_g) owing to the presence of the rigid pyrrolidone group [19, 31]. These rigid pyrrolidone groups can permit faster ionic mobility as compared to other semi-crystalline polymers. Another advantage of using PVP is that it can be thermally crosslinked resulting in the improved thermal stability and mechanical strength of the blend material [19]. It has been reported that the addition of salt to PVP with conducting species such as silver and potassium has a marked influence on its conductivity [32, 33]. Also, PVP has been reported to be the best candidate for humidity sensor in the presence of iodine and cobalt [34]. The presence of hydroxyl (OH) and carbonyl (C=O) groups in the side chains of PVA and PVP acts as the electron pair donors and enables complexations with lithium ions. Moreover, PVA and PVP form miscible blends because of the good compatibility between them. Both PVA and PVP are soluble in water and show a high degree of complexations with the wide range of inorganic salts [19].

The present work aimed at developing a new type of lithium ion conducting polymer blend electrolytes based on PVA and PVP complexed with lithium carbonate (Li_2CO_3) salt using solution casting method. The PVA/PVP/ Li_2CO_3 polymer blend electrolytes films have been characterized by FTIR, XRD, UV–vis, TGA, polarized optical microscopy (POM) and scanning electron microscopy (SEM). The impedance spectroscopy and dielectric studies were carried out in the frequency range 50 Hz–20 MHz and temperature range 40–150 °C. The influence of Li_2CO_3 salt on the structure, morphology, ionic conductivity and dielectric properties of polymer blend electrolytes have been investigated.

2 Experimental

2.1 Materials and methods

Poly (vinyl alcohol) of average molecular weight 125,000 g/mol with 86–89 % degree of hydrolysis was purchased from S. D. Fine Chemicals, Mumbai, India. Poly(*N*-vinyl pyrrolidone) of average molecular weight

40,000 g/mol was purchased from Sigma-Aldrich, India. Lithium carbonate (Li_2CO_3) of LR grade with the molecular weight of 73.89 g/mol was purchased from S.D. Fine Chemicals, Mumbai, India. Double distilled water was used as solvent throughout the study.

2.2 Preparation of PVA/PVP/ Li_2CO_3 polymer blend electrolyte films

A series of PVA/PVP/ Li_2CO_3 electrolyte films were prepared via traditional solution casting method with different concentrations of Li_2CO_3 salt varying from 0 to 25 wt% as shown in Table 1. PVA solutions were prepared separately by dissolving predetermined quantity of PVA powder in double-distilled water at 75 °C for 4 h. The required quantity of PVP was dissolved separately in double distilled water by continuous stirring for 2 h. PVA solution was added to PVP solution and stirred for 4 h. A required quantity (0–25 wt%) of Li_2CO_3 salt was also dissolved in distilled water by continuous stirring for 2 h and added to the PVA/PVP blend solution. PVA/PVP/ Li_2CO_3 electrolyte solution was further stirred for 6 h until the homogeneous mixer was achieved. The resulting PVA/PVP/ Li_2CO_3 electrolyte solution was poured into a glass Petri dish and dried at 60 °C for 8 h. The dried PVA/PVP/ Li_2CO_3 polymer blend electrolyte films were peeled off from the Petri dish and kept in the vacuum desiccators before using them for further study. The detailed protocol for the synthesis of PVA/PVP/ Li_2CO_3 polymer blend electrolyte films is represented in Fig. 1 and the possible interaction mechanism between the PVA/PVP blend and Li_2CO_3 salt is depicted in Fig. 2.

2.3 Characterizations

FTIR spectra of PVA/PVP/ Li_2CO_3 polymer blend electrolyte films in a transmittance mode were recorded using Fourier Transform Infrared Spectrophotometer (Shimadzu, IRAffinity-1, Japan) at room temperature. Sixty-four scans of each sample were recorded in the spectral region of 400–4000 cm^{-1} with an optical resolution of 4 cm^{-1} .

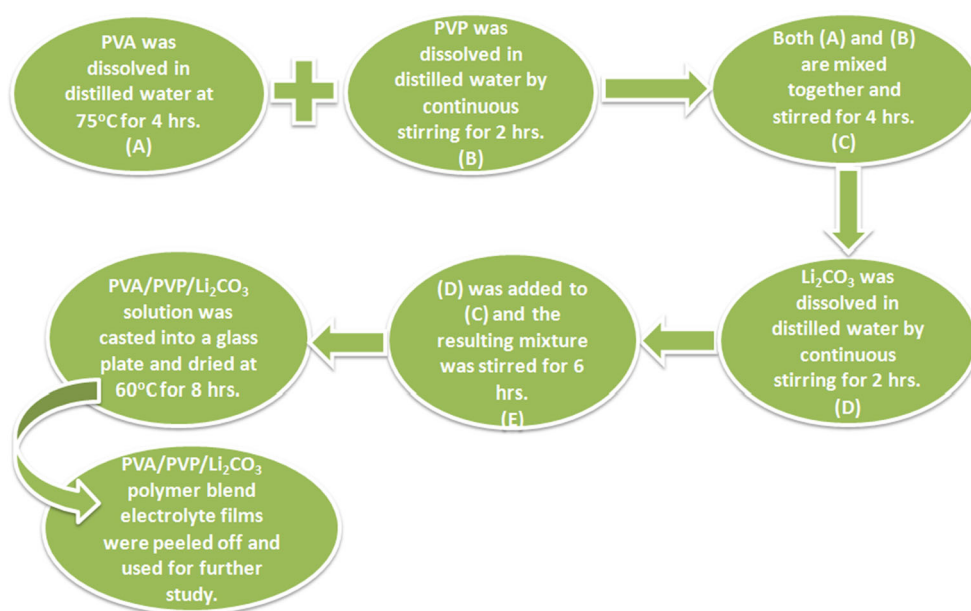
UV–vis absorption spectra of PVA/PVP/ Li_2CO_3 polymer blend electrolyte solutions were recorded using a Shimadzu UV-2401PC, UV–vis spectrophotometer in the wavelength range of 190–400 nm at room temperature.

X-ray diffraction patterns of PVA/PVP/ Li_2CO_3 polymer blend electrolyte films were recorded using Bruker AXS D8 focus advanced X-ray diffraction meter (Rigaku, Japan, Tokyo) at room temperature in the 2θ range from 10° to 80° using Cu $K\alpha$ radiation of wavelength $\lambda = 1.54060 \text{ \AA}$ generated at 40 kV and 20 mA. The samples were scanned with a scanning speed of 3°/min and the scanning step size of 0.005°/s.

Thermal stability of PVA/PVP/ Li_2CO_3 polymer blend electrolyte films was evaluated using Mettler Toledo, TGA/STDA851, thermogravimetric analyzer under N_2 atmosphere with α -alumina as reference material. The samples were heated from room temperature to 700 °C at the rate of 10 °C/min.

The surface morphology and the microstructures of PVA/PVP/ Li_2CO_3 polymer blend electrolyte films were examined using crossed polarizing optical microscope (Olympus BX-53, Singapore) at room temperature at a magnification of 10× and scanning electron microscope (Carl Zeiss EVO/18SH, UK) operated at an accelerating

Fig. 1 Protocol for the synthesis of PVA/PVP/ Li_2CO_3 polymer blend electrolytes films



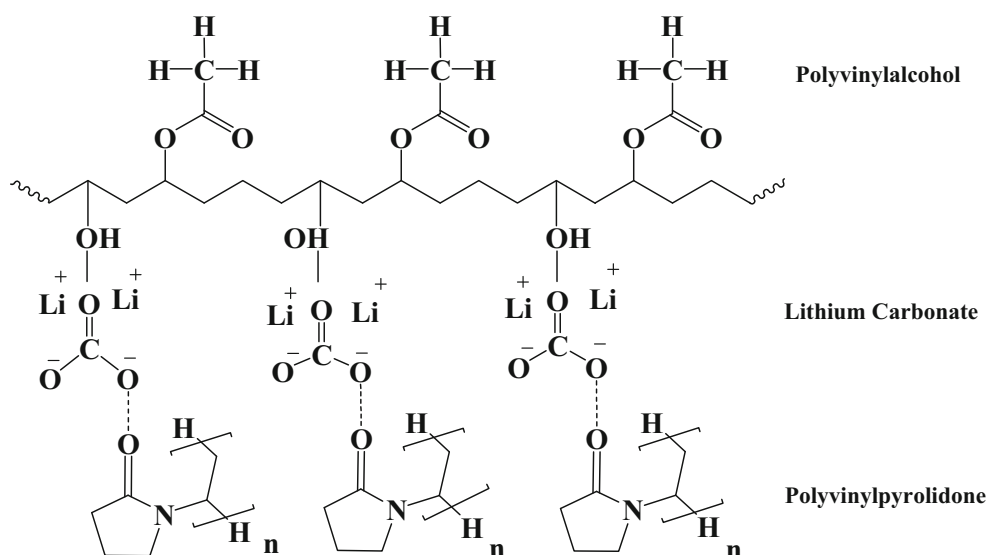


Fig. 2 Schematic representation of the possible interaction between polymers and the salt

voltage of 15 kV. Before SEM characterizations, the samples were sputtered with a layer of gold using a sputter coater in order to minimize sample charging effect due to an electron beam.

Contact angles of water droplets on the surfaces of PVA/PVP blend and PVA/PVP/Li₂CO₃ polymer blend electrolyte films were measured at room temperature using sessile drop method on contact angle goniometer (Ramehart 21 AC) equipped with a camera and monitor. Water drops of 5 μ l were carefully placed on the films using a micro-syringe and the contact angle measured at left and right sides of the drop. The obtained contact angle was the average value of ten readings.

The impedance spectroscopy and the dielectric studies of PVA/PVP/Li₂CO₃ polymer blend electrolyte films were recorded using Wayne Kerr 6500B (Chichester, West Sussex, UK) Precision Impedance Analyzer in the wide range of frequencies from 50 Hz to 20 MHz and temperature in the range 40–150 $^{\circ}$ C.

3 Results and discussions

3.1 FTIR spectroscopy

FTIR spectroscopy is a very useful technique for the investigation of polymer structures which provides information about the interactions and complexations between the various constituents of polymer electrolyte films. These interactions can induce changes in the vibrational modes of the polymer electrolytes [35]. The FTIR spectra of PVA/PVP blend and PVA/PVP/Li₂CO₃ polymer blend

electrolyte films are shown in Fig. 3a–f. The FTIR spectrum of PVA/PVP blend (50/50) film is depicted in Fig. 3a which shows the broad FTIR band around 3400 cm^{-1} which is attributed to –OH stretching vibration and a weak band at 2935 cm^{-1} corresponding to –CH stretching vibration. A characteristic band at 1082 cm^{-1} in the FTIR spectrum of PVA/PVP blend corresponds to the stretching vibration of C–O group. A strong band at 1654 cm^{-1} is attributed to the stretching vibration of C=O group of PVP [36]. The bands at 842 and 1415 cm^{-1} correspond to CH₂ bending and wagging vibrations respectively. The band at 1565 cm^{-1} attributed to C–N stretching vibrations of PVP

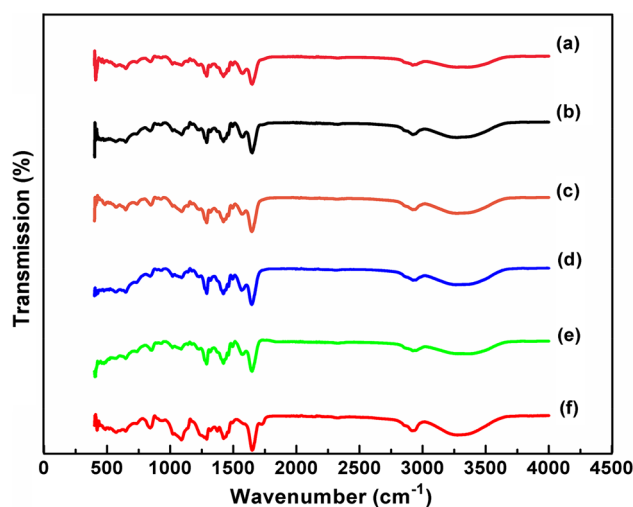


Fig. 3 FTIR spectra of PVA/PVP/Li₂CO₃ polymer blend electrolyte films. (a) PVA/PVP blend (b) 5 wt% Li₂CO₃, (c) 10 wt% Li₂CO₃, (d) 15 wt% Li₂CO₃, (e) 20 wt% Li₂CO₃, (f) 25 wt% Li₂CO₃

is also observed in the FTIR spectrum of PVA/PVP blend film. The FTIR spectrum of PVA/PVP blend film indicates the miscibility of both polymers which is due to hydrogen bonding interaction between hydroxyl groups of PVA and carbonyl group of PVP. The FTIR spectra of PVA/PVP blend films doped with different wt% of Li_2CO_3 salt is shown in Fig. 3b–f. The band around 3400 cm^{-1} shifts towards lower wavenumbers (3361 , 3354 , 3348 , 3334 and 3305 cm^{-1}) with the addition of Li_2CO_3 salt (5–25 wt%), indicating the interaction between Li^+ ions with hydroxyl groups of PVA and carbonyl groups of PVP. In addition, the bands at 2935 cm^{-1} which is attributed to $-\text{CH}$ stretching vibrations shifts towards lower wavenumbers with an increase in Li_2CO_3 doping. This indicates the variations in the anion conformations and coordination bond lengths to the Li^+ cations [19]. The band at 1565 cm^{-1} which is attributed to C–N stretching vibrations of PVP was disappeared when Li_2CO_3 doping was increased to 25 wt%. Thus, the changes in the existing peaks or their disappearance in the FTIR spectra of PVA/PVP/ Li_2CO_3 polymer blend electrolyte films are the direct evidence of complex formation between the polymers and Li_2CO_3 salt [37].

3.2 UV–vis spectroscopy

UV–visible spectroscopy is one of the most important techniques to study the optical absorption and in particular absorption edge which gives information about the band structure and the optical band gap energy for both crystalline and amorphous samples [38]. The UV–vis absorption spectra of PVA/PVP blend and Li_2CO_3 doped PVA/PVP blends are given in Fig. 4a–f. The UV–vis absorption spectrum of PVA/PVP blend shows an absorption band at

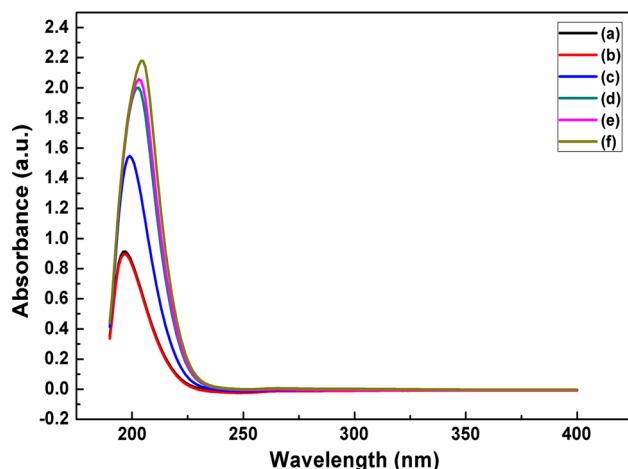


Fig. 4 UV–vis spectra of PVA/PVP/ Li_2CO_3 polymer blend electrolyte films. (a) PVA/PVP blend, (b) 5 wt% Li_2CO_3 , (c) 10 wt% Li_2CO_3 , (d) 15 wt% Li_2CO_3 , (e) 20 wt% Li_2CO_3 , (f) 25 wt% Li_2CO_3

197 nm which arises due to carbonyl group containing segments and are assigned to localized $n-\pi^*$ transitions. It was also observed that the Li_2CO_3 doped PVA/PVP blends showed higher absorption than pure PVA/PVP blends which means that the absorption of PVA/PVP/ Li_2CO_3 polymer blend electrolyte has increased with increasing the Li_2CO_3 content [39]. In addition, the absorption band is shifted towards higher wavelength for PVA/PVP/ Li_2CO_3 polymer blend electrolyte with 25 wt% Li_2CO_3 content. The shift of the absorption bands towards higher wavelength is due to the formation of charge transfer transitions via inter and intra-molecular hydrogen bonding between Li^+ ions, hydroxyl groups of PVA and carbonyl groups of PVP [40].

3.3 X-ray diffraction studies

The X-ray diffraction (XRD) patterns of pure Li_2CO_3 salt, PVA/PVP blend and PVA/PVP/ Li_2CO_3 polymer blend electrolyte films are displayed in Fig. 5a–g. The XRD pattern of Li_2CO_3 salt (Fig. 5a) exhibits sharp peaks at 2θ angle of 21.30° ($d = 4.16\text{ \AA}$), 23.39° ($d = 3.79\text{ \AA}$), 29.39° ($d = 3.03\text{ \AA}$), 30.54° ($d = 2.92\text{ \AA}$), 31.71° ($d = 2.81\text{ \AA}$), 34.03° ($d = 2.63\text{ \AA}$), 36.02° ($d = 2.49\text{ \AA}$), 36.89° ($d = 2.43\text{ \AA}$), 39.53° ($d = 2.27\text{ \AA}$) and 48.68° ($d = 1.86\text{ \AA}$) which indicates crystalline nature of the salt [41]. The XRD pattern of PVA/PVP blend film (Fig. 5b) shows two amorphous halos at $2\theta = 19.28^\circ$ and $2\theta = 30.45^\circ$ which are attributed to the (101) and (020) crystal planes respectively. The XRD pattern of PVA/PVP/ Li_2CO_3 polymer blend electrolyte films also shows two amorphous halos similar to the XRD pattern of PVA/PVP blend film. The XRD patterns of PVA/PVP/ Li_2CO_3 polymer

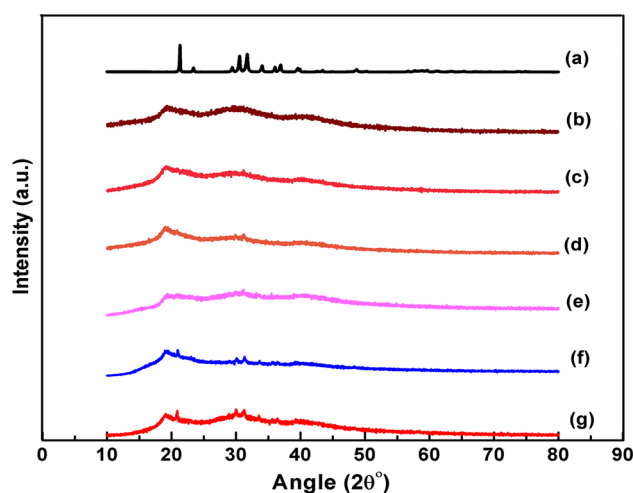


Fig. 5 X-ray diffraction pattern of PVA/PVP/ Li_2CO_3 polymer blend electrolyte films. (a) Li_2CO_3 powder, (b) PVA/PVP blend, (c) 5 wt% Li_2CO_3 , (d) 10 wt% Li_2CO_3 , (e) 15 wt% Li_2CO_3 , (f) 20 wt% Li_2CO_3 , (g) 25 wt% Li_2CO_3

blend electrolyte films infer that lithium salt has a significant effect on the ordered arrangement of the polymer chains which can result in the enhancement of ionic conductivity [3]. The sharp peaks corresponding to Li_2CO_3 salt were almost disappeared in the polymer blend electrolyte films which indicate that Li_2CO_3 salt was completely dissolved in the PVA/PVP blend matrix. However, at higher doping concentration (20 and 25 wt%) of Li_2CO_3 salt, the PVA/PVP/ Li_2CO_3 polymer blend electrolyte films shows less intense diffraction peak at 21.30° corresponding to d-spacing of 4.16 \AA for Li_2CO_3 salt. The absence of sharp diffraction peak in the electrolyte films suggest that the amorphous phase is dominant which can results in a greater ionic diffusivity with high ionic conductivity [28, 42, 43]. Thus, the XRD results indicate the complex formation between the Li_2CO_3 salt and PVA/PVP blend matrix [44]. Similar results were obtained for other polymers upon addition of salts as well as inorganic fillers [45, 46].

3.4 Thermal analysis

Thermal stability of polymer blend electrolytes is one of the key parameters for their practical applications in lithium ion batteries. In order to determine the thermal stability of the prepared electrolyte films, the thermogravimetric analysis (TGA) was carried out. The TGA thermograms of PVA/PVP blend and PVA/PVP/ Li_2CO_3 polymer blend electrolyte films doped with the various mass fraction of Li_2CO_3 salt are depicted in Fig. 6a–e. It can be seen that the decomposition of PVA/PVP blend and PVA/PVP/ Li_2CO_3 polymer blend electrolyte films occur in three steps. The first step of decomposition was observed at the temperature slightly below 100°C which could be attributed to the evaporation of superficial or residual moisture in the sample [3]. The second step of decomposition was observed in the

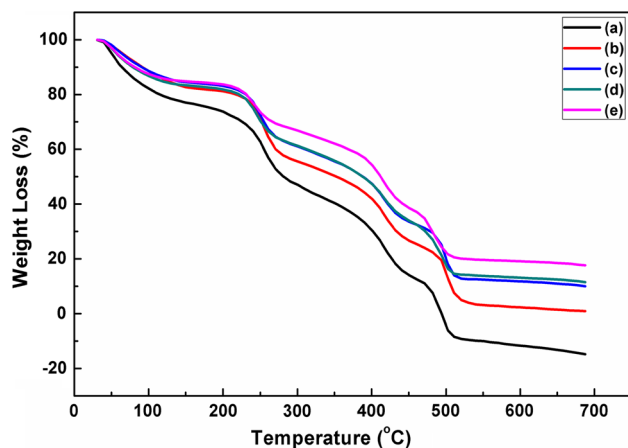


Fig. 6 TGA thermograms of PVA/PVP/ Li_2CO_3 polymer blend electrolyte films. (a) PVA/PVP blend, (b) 5 wt% Li_2CO_3 , (c) 10 wt% Li_2CO_3 , (d) 15 wt% Li_2CO_3 , (e) 20 wt% Li_2CO_3

temperature range $100\text{--}240^\circ\text{C}$ which can be attributed to the decomposition of the main chain of polymers [35]. The third step of decomposition was observed in the region $240\text{--}350^\circ\text{C}$ which could be attributed to the decomposition of Li_2CO_3 salt. With the incorporation of Li_2CO_3 salt in the PVA/PVP blend matrix, less weight loss was observed in the PVA/PVP/ Li_2CO_3 polymer blend electrolyte films indicating the enhanced thermal stability of polymer blend electrolytes. The observed thermal stability ($\sim 240^\circ\text{C}$) of polymer blend electrolytes is sufficient enough for their potential application as electrolyte material in lithium ion rechargeable batteries.

3.5 Surface morphology

Polarized optical microscopy (POM) and scanning electron microscopy (SEM) was employed to elucidate the microstructure and the surface morphology of PVA/PVP/ Li_2CO_3 polymer blend electrolyte films. The POM and SEM micrographs of PVA/PVP blend and PVA/PVP/ Li_2CO_3 polymer blend electrolyte films are given in Figs. 7 and 8 respectively. For pure PVA/PVP blend film, a smooth uniform surface morphology can be seen in both optical and scanning electron micrographs. The addition of Li_2CO_3 salt in PVA/PVP blend results in a typical spherulitic texture of PVA/PVP/ Li_2CO_3 polymer blend electrolyte films. The spherulitic texture in the electrolyte film represents the lamellar crystalline nature and the dark boundaries between them indicate the amorphous content in the sample [3]. The amorphous phase occupied the regions between the lamella so that the spherulites are embedded in the amorphous matrix [31, 47]. Also, the XRD analysis infers that the amorphous region is more dominant in the polymer blend electrolytes. Thus, the optical and scanning electron microscopy results are in concordance with FTIR and XRD results.

3.6 Contact angle measurements

The surface characteristics of PVA/PVP blend and PVA/PVP/ Li_2CO_3 polymer blend electrolyte films were further

Table 1 Feed compositions for PVA/PVP/ Li_2CO_3 polymer blends electrolyte films

PVA (wt%)	PVP (wt%)	Li_2CO_3 (wt%)
50	50	0
45	50	5
40	50	10
35	50	15
30	50	20
25	50	25

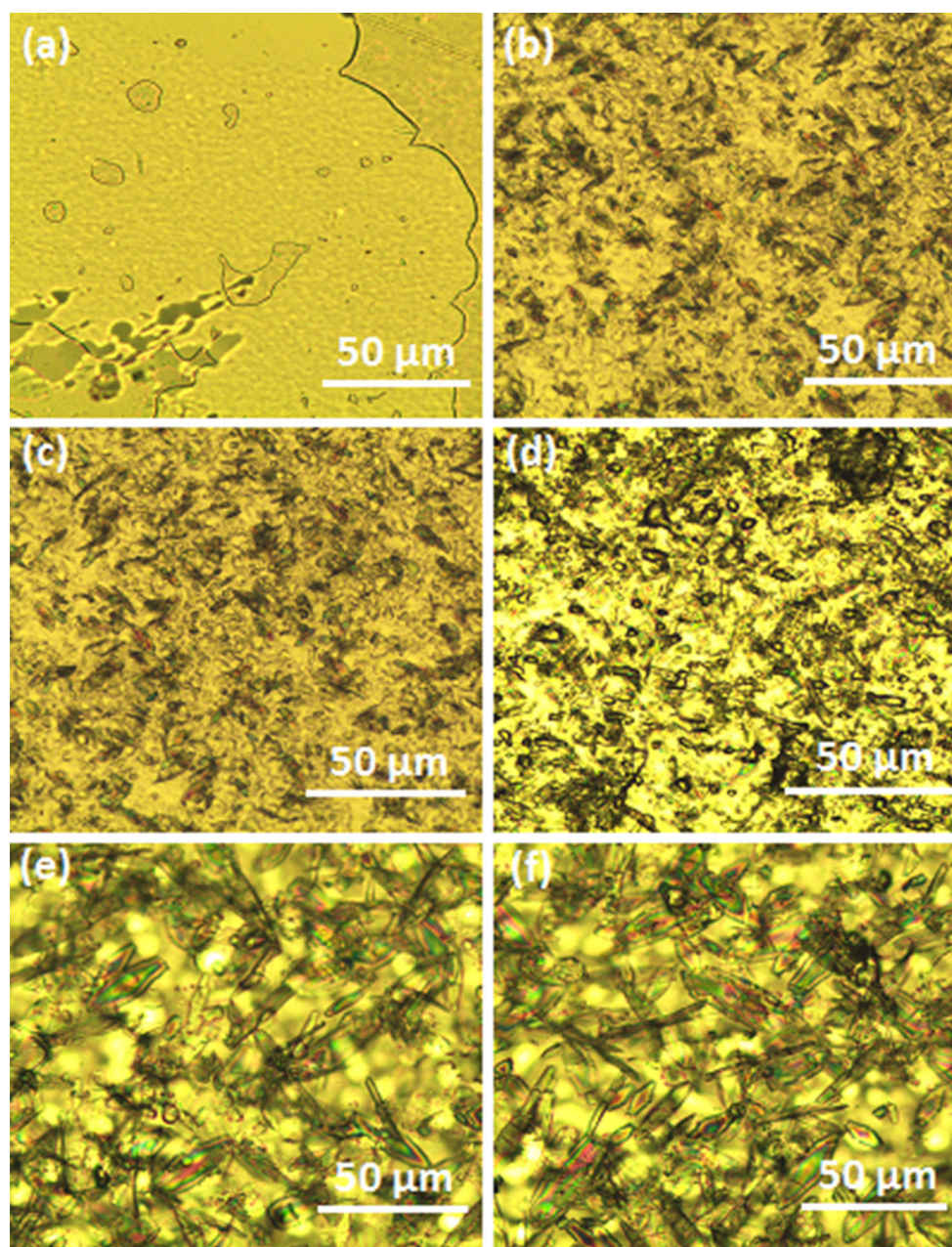


Fig. 7 Optical microscopy images of PVA/PVP/Li₂CO₃ polymer blend electrolyte films. **a** PVA/PVP blend, **b** 5 wt% Li₂CO₃, **c** 10 wt% Li₂CO₃, **d** 15 wt% Li₂CO₃, **e** 20 wt% Li₂CO₃, **f** 25 wt% Li₂CO₃

evaluated by measuring their water contact angles. The water contact angles on the surfaces of PVA/PVP blend and PVA/PVP/Li₂CO₃ polymer blend electrolyte films were measured at room temperature and the results are shown in Fig. 9. Table 2 summarizes the results (surface energy and work of adhesion) obtained from contact angle measurements. The contact angle of water for PVA/PVP blend film was found to be $57.08 \pm 0.04^\circ$ (Fig. 9a) while that of PVA/PVP/Li₂CO₃ polymer blend electrolyte film with 25 wt% Li₂CO₃ salt content (Fig. 9f) was found to be

$24.30^\circ \pm 0.52^\circ$. This indicates that the hydrophilicity of electrolyte film has increased which could be due to the hydrophilic nature of polymers and Li₂CO₃ salt. On the other hand, the surface energy for PVA/PVP blend film was found to be $49.59 \pm 0.02 \text{ mJ/m}^2$ (Table 2) while that of PVA/PVP/Li₂CO₃ polymer blend electrolyte film with 25 wt% Li₂CO₃ salt content was found to be $67.01 \pm 0.22 \text{ mJ/m}^2$. This indicates that the surface energy of PVA/PVP blend films has improved with an increase in the Li₂CO₃ salt content. In addition, the work of adhesion

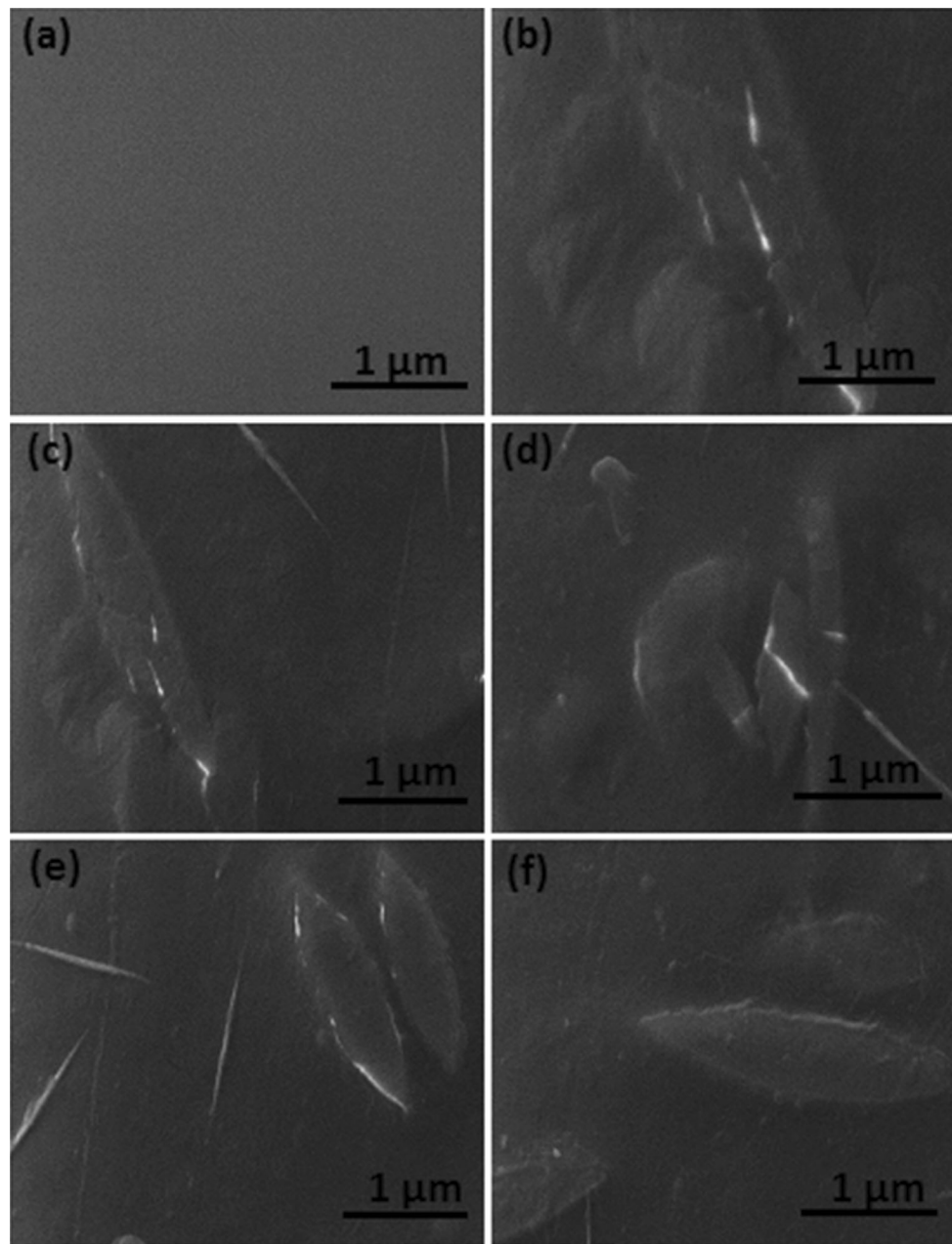


Fig. 8 SEM micrographs of PVA/PVP/Li₂CO₃ polymer blend electrolyte films. **a** PVA/PVP blend, **b** 5 wt% Li₂CO₃, **c** 10 wt% Li₂CO₃, **d** 15 wt% Li₂CO₃, **e** 20 wt% Li₂CO₃, **f** 25 wt% Li₂CO₃

was also calculated from contact angle values using the formula given in our previous work [48]. The work of adhesion for PVA/PVP blend film was calculated to be 111.08 mJ/m² while that of PVA/PVP/Li₂CO₃ polymer blend electrolyte film with 25 wt% Li₂CO₃ salt content was calculated to be 137.56 mJ/m². Thus, from the contact angle measurements, it can be concluded that the addition of Li₂CO₃ salt in PVA/PVP blends have the notable effect on the surface characteristics of polymer blend electrolyte films.

3.7 Impedance spectroscopy

Impedance spectroscopy is a very powerful and widely used technique to study electrical properties of electrolyte materials and their interfaces with electronically conducting electrodes. The shape of impedance spectra of a material gives information about the electrode polarization and about the current carriers, whether they are electrons or ions. The complex impedance plots (plots between real (Z') and imaginary (Z'') parts of impedance) for PVA/PVP/

Fig. 9 Contact angles of water on PVA/PVP/Li₂CO₃ polymer blend electrolyte films. **a** PVA/PVP blend, **b** 5 wt% Li₂CO₃, **c** 10 wt% Li₂CO₃, **d** 15 wt% Li₂CO₃, **e** 20 wt% Li₂CO₃, **f** 25 wt% Li₂CO₃

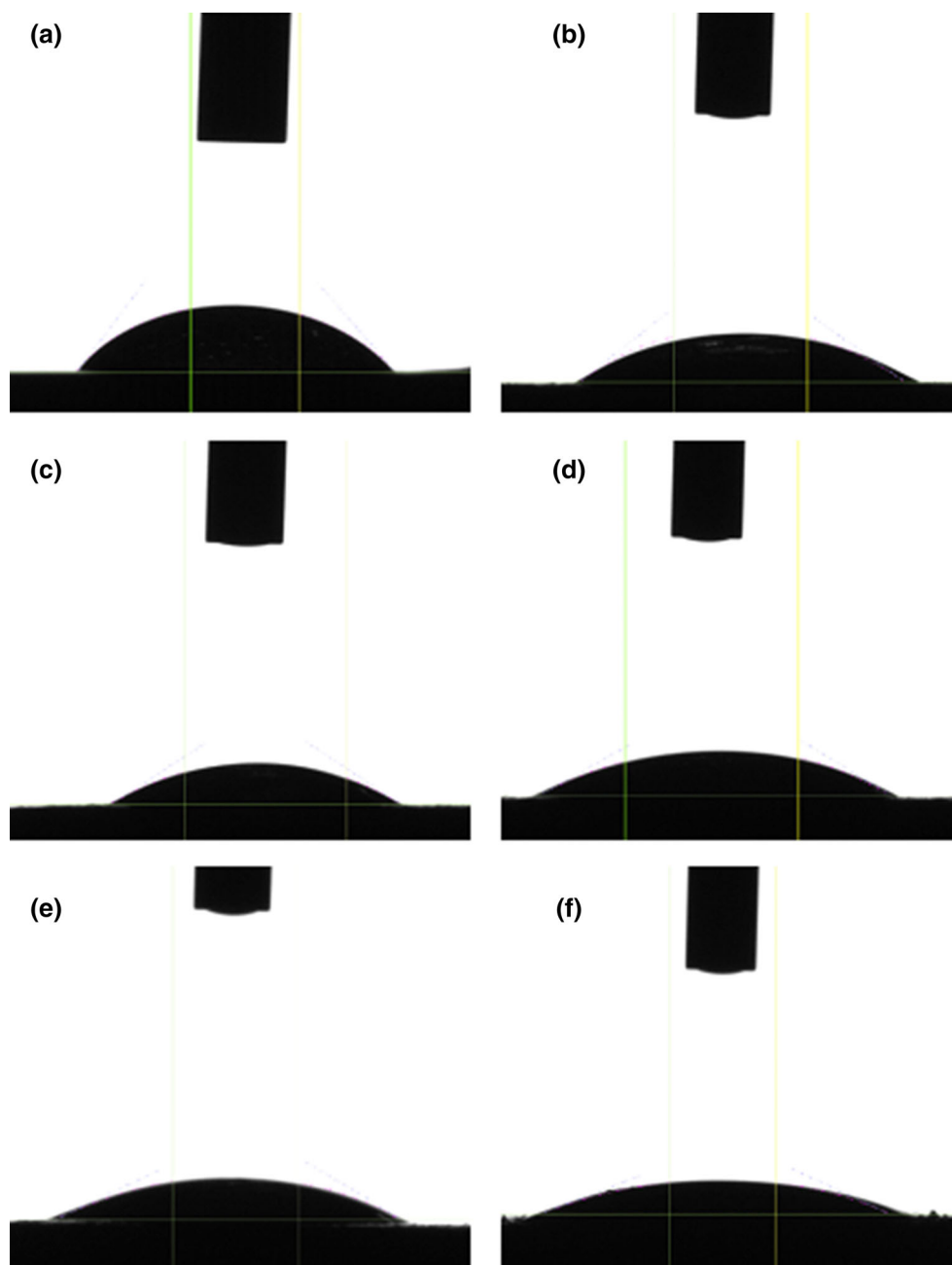


Table 2 Contact angle, surface energy and work of adhesion for PVA/PVP blend and PVA/PVP/Li₂CO₃ polymer blends electrolyte films

Li ₂ CO ₃ content (wt%)	Contact angle θ (°)	Surface energy (mJ/m ²)	Work of adhesion (mJ/m ²)
0	57.08 ± 0.04	49.59 ± 0.02	111.08
5	41.24 ± 0.48	58.70 ± 0.26	126.08
10	37.40 ± 0.14	60.76 ± 0.07	129.14
15	31.20 ± 0.25	63.06 ± 0.25	132.87
20	29.79 ± 0.31	64.58 ± 0.15	134.42
25	24.30 ± 0.52	67.01 ± 0.22	137.56

Li_2CO_3 polymer blend electrolyte films at different temperatures is shown in Fig. 10a–f. A typical Cole–Cole plot of PVA/PVP/ Li_2CO_3 polymer blend electrolyte films with 0, 5, 10, 15 and 25 wt% of Li_2CO_3 consist of a broadened semicircular portion in the high-frequency region which is mainly due to a parallel combination of geometrical

capacitor (C_g) and the bulk resistor (R) [49]. For PVA/PVP/ Li_2CO_3 polymer blend electrolyte film with 20 wt% Li_2CO_3 salt the Cole–Cole plots (Fig. 10e) shows a depressed semicircular portion in the high frequency region which can be related to charge transfer process and a spike in the low frequency region which is a characteristic of

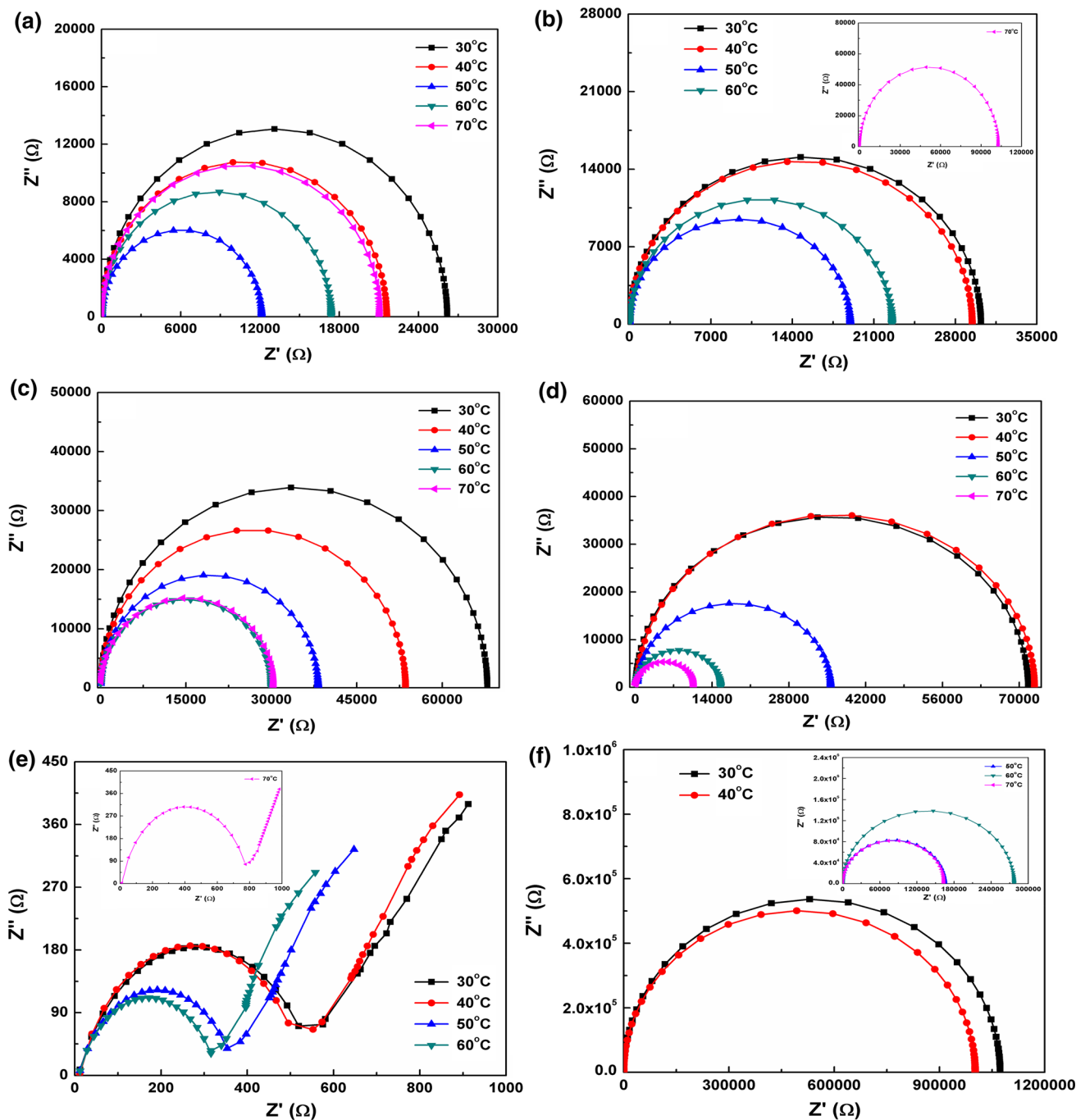


Fig. 10 a Cole–Cole plot for PVA/PVP blend film. b Cole–Cole plot for PVA/PVP/ Li_2CO_3 polymer blend electrolyte film with 5 wt% Li_2CO_3 . c Cole–Cole plot for PVA/PVP/ Li_2CO_3 polymer blend electrolyte film with 10 wt% Li_2CO_3 . d Cole–Cole plot for PVA/PVP/

Li_2CO_3 polymer blend electrolyte film with 15 wt% Li_2CO_3 . e Cole–Cole plot for PVA/PVP/ Li_2CO_3 polymer blend electrolyte film with 20 wt% Li_2CO_3 . f Cole–Cole plot for PVA/PVP/ Li_2CO_3 polymer blend electrolyte film with 25 wt% Li_2CO_3

diffusion process [44, 50, 51]. The depressed semicircle indicates that the relaxation of ions is non-Debye in nature. The low-frequency spikes indicate the presence of double layer capacitance at the electrode/sample interface [52]. The intercept of the semicircle with the real axis (Z') gives the value of the bulk ionic resistance (R_b) of the polymer blend electrolytes. From Cole–Cole plots, it can be seen that as the temperature increases the diameter of the semicircle decreases which implies that the bulk resistance (R_b) decreases. By knowing the bulk resistance (R_b) and the sample dimensions, the ionic conductivity of polymer blend electrolytes can be calculated using the equation:

$$\sigma = L/R_b A \quad (1)$$

where σ is the ionic conductivity, R_b is the bulk resistance, L is the film thickness and A is the area of an electrode. It is well known that the conductivity occurs only in the amorphous region of the polymer electrolyte. Therefore, the high ionic conductivity can be expected for highly amorphous polymer electrolytes [3]. The ionic conductivity as a function of Li_2CO_3 concentration at room temperature (30 °C) is shown in Fig. 11. The dependence of conductivity on the salt concentration indicates the specific interaction between the polymer matrix and the salt. It was observed that the conductivity increases from $5.58 \times 10^{-9} \text{ S cm}^{-1}$ for PVA/PVP blend film to $1.15 \times 10^{-5} \text{ S cm}^{-1}$ for 20 wt% Li_2CO_3 in the polymer electrolytes. The increase in ionic conductivity with increase in Li_2CO_3 concentration can be attributed to an increased ionic mobility and ionic charge carrier concentrations [38]. The increase in the ionic conductivity can be attributed to the interaction of Li^+ ions with hydroxyl group of PVA and carbonyl group of PVP which forms charge transfer complexes and acts as hopping sites for Li^+ ions to migrate into PVA/PVP blend and expected to

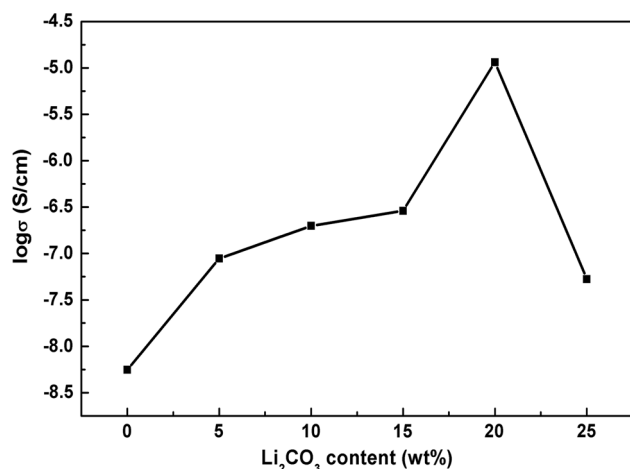


Fig. 11 Variation of ionic conductivity as a function of salt concentration in PVA/PVP/ Li_2CO_3 blend electrolytes

reduce the trapping sites to create path through the amorphous phase of the polymer matrix and this favours the ionic conductivity [53]. Also, it can be seen that the ionic conductivity decreases at higher salt concentration, i.e. at 25 wt% of Li_2CO_3 . This could be due to the influence of ion pairs, ion triplets and the ion aggregations which reduces the overall mobility and the number of effective charge carriers. These results are in concordance with several other results reported by various researchers on different polymer electrolyte systems [54, 55].

3.8 Dielectric properties

The dielectric measurements are very useful in obtaining information about the ion-polymer interaction and conduction mechanism in polymer electrolyte systems. The dielectric properties such as dielectric constant (ϵ) and dielectric loss ($\tan \delta$) of PVA/PVP blend and PVA/PVP/ Li_2CO_3 polymer blend electrolyte films were evaluated using impedance analyzer at various frequencies (50 Hz - 20 MHz) and temperatures (40–150 °C). Table 3 gives the summary of dielectric data for PVA/PVP blend and PVA/PVP/ Li_2CO_3 polymer blend electrolyte films. Figure 12a–f shows the dielectric constant plots for PVA/PVP blend and PVA/PVP/ Li_2CO_3 polymer blend electrolyte films with different content of Li_2CO_3 salt. The high values of dielectric constant were observed at the low-frequency region which is mainly ascribed to the Maxwell–Wagner ionic conduction and electrode polarization effect resulting from the accumulation of ions at the electrode–electrolyte interface [56, 57]. As the frequency increases, the dielectric constant begins to decrease and attain a constant value at higher frequencies. This is because the periodic reversal of electric field is so fast that there was no excess ion diffusion in the direction of an electric field [58] and most of the ions are in the bulk of the sample, leading to decrease in the dielectric constant value with increase in frequency [59]. These results imply that PVA/PVP/ Li_2CO_3 polymer blend electrolyte system show a non-Debye type of behaviour where the space charge regions with respect to frequency

Table 3 Dielectric constant and dielectric loss tangent ($\tan \delta$) of PVA/PVP blend and PVA/PVP/ Li_2CO_3 polymer blends electrolyte films

Li_2CO_3 content (wt%)	Dielectric constant (ϵ)	Dielectric loss (Tan δ)
0	18.22, 50 Hz, 150 °C	2.16, 50 Hz, 150 °C
5	99.55, 50 Hz, 150 °C	2.97, 50 Hz, 150 °C
10	128.98, 50 Hz, 150 °C	3.45, 50 Hz, 150 °C
15	139.84, 50 Hz, 150 °C	3.58, 50 Hz, 150 °C
20	628.34, 50 Hz, 150 °C	3.66, 50 Hz, 150 °C
25	1201.57, 50 Hz, 150 °C	3.94, 50 Hz, 150 °C

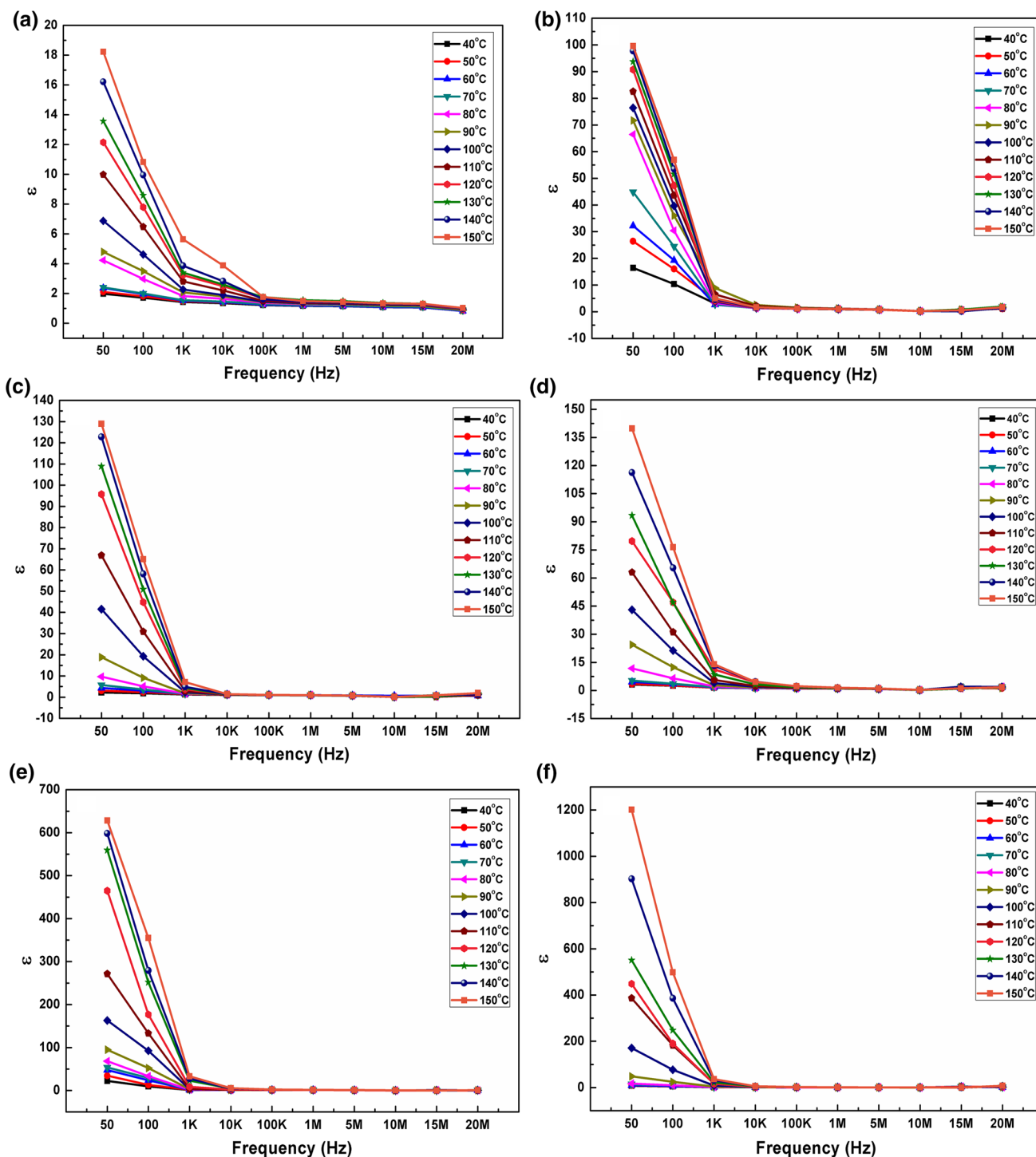


Fig. 12 **a** Dielectric constant plot for PVA/PVP blend film. **b** Dielectric constant plot for PVA/PVP/ Li_2CO_3 polymer blend electrolyte film with 5 wt% Li_2CO_3 . **c** Dielectric constant plot for PVA/PVP/ Li_2CO_3 polymer blend electrolyte film with 10 wt% Li_2CO_3 . **d** Dielectric constant plot for PVA/PVP/ Li_2CO_3 polymer blend

electrolyte film with 15 wt% Li_2CO_3 . **e** Dielectric constant plot for PVA/PVP/ Li_2CO_3 polymer blend electrolyte film with 20 wt% Li_2CO_3 . **f** Dielectric constant plot for PVA/PVP/ Li_2CO_3 polymer blend electrolyte film with 25 wt% Li_2CO_3

are explained in terms of ion diffusion [60]. The dielectric constant also increases with increase in the Li_2CO_3 content. The high value of dielectric constant for PVA/PVP/ Li_2CO_3

polymer blend electrolyte film with 25 wt% Li_2CO_3 salt can be attributed to the enhanced charge carrier density at the space charge accumulation region, resulting in an

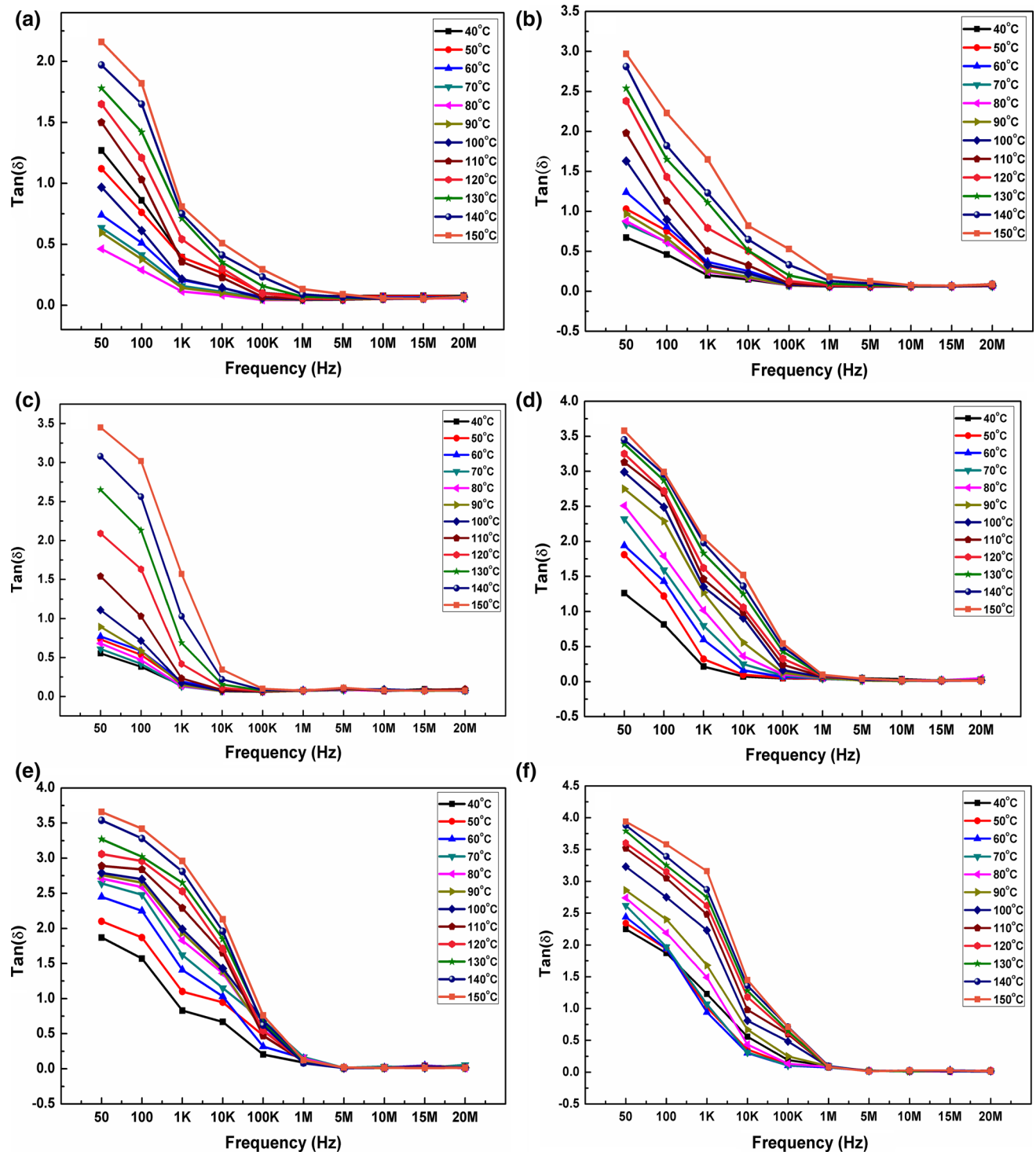


Fig. 13 **a** Dielectric loss ($\tan \delta$) plot for PVA/PVP blend film. **b** Dielectric loss ($\tan \delta$) plot for PVA/PVP/ Li_2CO_3 polymer blend electrolyte film with 5 wt% Li_2CO_3 . **c** Dielectric loss ($\tan \delta$) plot for PVA/PVP/ Li_2CO_3 polymer blend electrolyte film with 10 wt% Li_2CO_3 . **d** Dielectric loss ($\tan \delta$) plot for PVA/PVP/ Li_2CO_3 polymer

blend electrolyte film with 15 wt% Li_2CO_3 . **e** Dielectric loss ($\tan \delta$) plot for PVA/PVP/ Li_2CO_3 polymer blend electrolyte film with 20 wt% Li_2CO_3 . **f** Dielectric loss ($\tan \delta$) plot for PVA/PVP/ Li_2CO_3 polymer blend electrolyte film with 25 wt% Li_2CO_3

increase in the equivalent capacitance value. The dielectric constant also increases with the increase in temperature at lower frequency region which indicates enhancement of

free ion motion within the polymer matrix and increase in the mobility of the ions [53]. Another reason for the increase in the dielectric constant would be the presence of

amorphous and crystalline regions in PVA/PVP matrix which acts as hopping centres for charge carriers. With an increase in temperature, the crystalline phase of polymer matrix dissolves progressively into amorphous phase with the increase in temperature. This, in turn, influences the hopping and thus increases the dielectric constant [53]. This behaviour is typical of polar dielectrics because dipole orientation is facilitated by increasing the temperature, thus increasing the dielectric constant [61]. The variation of dielectric loss ($\tan \delta$) with frequency and temperature for PVA/PVP blend and PVA/PVP/Li₂CO₃ polymer blend electrolyte films is shown in Fig. 13a–f. The dielectric loss is the ratio of the loss factor to the relative dielectric constant. It is a measure of the electric energy lost to the energy stored in a periodic field. The samples showed high dielectric loss values at low frequencies and as the frequency increases the dielectric loss decreases. The high dielectric loss at the low-frequency region is due to an accumulation of free charge carriers at the interface between the electrolyte and the electrodes [62]. In other words, the high values of dielectric loss at low-frequency region are due to conduction loss as well as electrode polarization. At higher frequencies, the polar ionization due to charge accumulation decreases leading to a decrease in the dielectric loss value. The dielectric loss also increases with increase in the Li₂CO₃ content which could be attributed to the more localization of charge carriers along with the mobile ions causing higher ionic conductivity [63, 64].

4 Conclusions

New PVA/PVP/Li₂CO₃ solid polymer blend electrolytes with different compositions have been prepared by solution casting method. The FTIR, XRD and UV–vis absorption spectroscopy studies confirm the complex formation of PVA/PVP blend matrix with Li₂CO₃ salt. The TGA results indicate an enhancement in the thermal stability of polymer blend electrolytes. The contact angle measurements reveal that the addition of Li₂CO₃ salt in PVA/PVP blends have the notable effect on the surface characteristics of polymer blend electrolyte films. The complex impedance plots (Cole–Cole plots) indicate that PVA/PVP blend can be effectively doped with Li₂CO₃ to enhance its conductivity. The ionic conductivity of polymer blend electrolytes increases with increase in the Li₂CO₃ concentration. The increase in conductivity with increase in salt concentration can be attributed to the formation of charge transfer complexes. The highest ionic conductivity of 1.15×10^{-5} S cm⁻¹ at 30 °C has been observed for PVA/PVP/Li₂CO₃ polymer blend electrolytes with 20 wt% Li₂CO₃ content. The dielectric results revealed the non-Debye type of

behaviour. The dielectric constant as high as 1200 ($\epsilon = 1201.57$, 50 Hz, 150 °C) and the dielectric loss well below 4 ($\tan \delta = 3.94$, 50 Hz, 150 °C) were obtained for polymer blend electrolytes with 25 wt% Li₂CO₃ salt. Thus, the results obtained in the present study suggest that the PVA/PVP/Li₂CO₃ polymer blend electrolyte system seems to be a promising candidate for solid state battery applications.

Acknowledgments Kalim Deshmukh is grateful to the management of B. S. Abdur Rahman University, Chennai-600048, TN, India for providing Junior Research Fellowship (JRF) to carry out this research work.

References

1. S. Giddey, S.P.S. Badwal, *Ionics* **19**, 523–528 (2013)
2. P.K. Singh, K.W. Kim, H.W. Rhee, *Electrochem. Commun.* **11**, 1247–1250 (2009)
3. A.R. Polu, D.K. Kim, H.W. Rhee, *Ionics* **21**, 2771–2780 (2015)
4. J. Qiao, T. Hamaya, T. Okada, *Polymer* **46**, 10809–10816 (2005)
5. J.B. Goodenough, K.S. Park, *J. Am. Chem. Soc.* **135**, 1167–1176 (2013)
6. D.Y. Park, D.Y. Park, Y. Lan, Y.S. Lim, M.S. Kim, *J. Ind. Eng. Chem.* **15**, 588–594 (2009)
7. R.C. Agrawal, G.P. Pandey, *J. Phys. D Appl. Phys.* **41**, 223001–223018 (2008)
8. J.M. Tarascon, M. Armand, *Nature* **414**, 359–367 (2001)
9. R. Singh, B. Bhattacharya, H.W. Rhee, P.K. Singh, *Int. Hydrogen Energy* **40**, 9365–9372 (2015)
10. A.R. Polu, H.W. Rhee, *Sci. Adv. Mater.* **8**, 931–940 (2016)
11. J. Zhang, B. Sun, X. Xuang, S. Chen, G. Wang, *Sci. Rep.* **4**, 6007–6013 (2014)
12. A.R. Polu, H.W. Rhee, *J. Ind. Eng. Chem.* **37**, 347–353 (2016)
13. A.R. Polu, R. Kumar, *Bull. Mater. Sci.* **37**, 309–314 (2014)
14. K.P. Radha, S. Selvasekarapandian, S. Karthikeyan, M. Hema, C. Sanjeeviraja, *Ionics* **19**, 1437–1447 (2013)
15. A.R. Polu, H.W. Rhee, D.K. Kim, *J. Mater. Sci.: Mater. Electron.* **26**, 8548–8554 (2015)
16. S.M. Pawde, K. Deshmukh, S. Parab, *J. Appl. Polym. Sci.* **109**, 1328–1337 (2008)
17. N. Rajeshwari, S. Selvasekarapandian, S. Karthikeyan, C. Sanjeeviraja, Y. Iwai, J. Kawamura, *Ionics* **19**, 1105–1113 (2013)
18. Y. Xiong, Q.L. Liu, Q.G. Zhang, A.M. Zhu, *J. Power Sources* **183**, 447–453 (2008)
19. A.R. Polu, R. Kumar, H.W. Rhee, *Ionics* **21**, 125–132 (2015)
20. S.M. Pawde, K. Deshmukh, *J. Appl. Polym. Sci.* **109**, 3431–3437 (2008)
21. K. Deshmukh, J. Ahmad, M.B. Hagg, *Ionics* **20**, 957–967 (2014)
22. A. Rocco, R.P. Pereira, M.I. Felisberti, *Polymer* **42**, 5199–5205 (2001)
23. J. Ahmad, K. Deshmukh, M. Habib, M.B. Hagg, *Arab. J. Sci. Eng.* **39**, 6805–6814 (2014)
24. J. Ahmad, K. Deshmukh, M.B. Hagg, *Int. J. Polym. Anal. Charact.* **18**, 287–296 (2013)
25. K. Deshmukh, M.B. Ahamed, R.R. Deshmukh, S.K.K. Pasha, K.K. Sadasivuni, D. Ponnamma, K. Chidambaram, *Eur. Polym. J.* **76**, 14–27 (2016)
26. K. Deshmukh, M.B. Ahamed, S.K.K. Pasha, R.R. Deshmukh, P.R. Bhagat, *RSC Adv.* **5**, 61933–61945 (2015)
27. S. Rajendran, M. Sivakumar, R. Subadevi, *Solid State Ionics* **167**, 335–339 (2004)

28. A.A. Mohamad, N.S. Mohamed, M.Z.A. Yahya, R. Othman, S. Ramesh, Y. Alias, A.K. Arof, *Solid State Ionics* **156**, 171–177 (2003)
29. C.C. Yang, S.J. Lin, G.M. Wu, *Mater. Chem. Phys.* **92**, 251–255 (2005)
30. Y. Pavani, M. Ravi, S. Bhavani, A.K. Sharma, V.V.R.N. Rao, *Polym. Eng. Sci.* **52**, 1685–1692 (2012)
31. N. Vijaya, S. Selvasekarapandian, G. Hirankumar, S. Karthikeyan, H. Nithya, C.S. Ramya, M. Prabu, *Ionics* **18**, 91–99 (2012)
32. N. Kumar, T. Sreekanth, M. Jaipal Reddy, U.V. Subba Rao, *J. Power Source* **101**, 130–133 (2001)
33. M. Jaipal Reddy, T. Sreekanth, M. Chandrashekar, U.V. Subba Rao, *J. Mater. Sci.* **35**, 2841–2845 (2000)
34. A.A.A. DeQueiroz, D.A.W. Soares, P. Trzesniak, G.A. Abraham, *J. Polym. Sci. B: Polym. Phys.* **39**, 459–469 (2001)
35. K. Deshmukh, M.B. Ahamed, R.R. Deshmukh, P.R. Bhagat, S.K.K. Pasha, A. Bhagat, R. Shirbhate, F. Telare, C. Lakhani, *Polym. Plast. Tech. Eng.* **55**, 231–241 (2016)
36. E.M. Abdelrazek, I.S. Elashmawi, H.M. Ragab, *Phys. B* **403**, 3097–3104 (2008)
37. A.R. Polu, H.W. Rhee, *J. Ind. Eng. Chem.* **31**, 323–329 (2015)
38. R.F. Bhajantari, V. Ravindrachary, V. Crasta, S.P. Nayak, B. Poojary, *Polymer* **47**, 3591–3598 (2006)
39. S.M. Pawde, K. Deshmukh, *J. Appl. Polym. Sci.* **110**, 2569–2578 (2008)
40. S.M. Pawde, K. Deshmukh, *J. Appl. Polym. Sci.* **114**, 2169–2179 (2009)
41. M. Sulaiman, A.A. Rahman, N.S. Mohamed, *Ionics* **22**, 327–332 (2016)
42. V.M. Mohan, V. Raja, A.K. Sharma, V.V.R.N. Rao, *Mater. Chem. Phys.* **94**, 177–181 (2005)
43. P.B. Bhargav, V.M. Mohan, A.K. Sharma, V.V.R.N. Rao, *Int. J. Polym. Mater.* **56**, 579–591 (2007)
44. G.B. Appetecchi, W. Henderson, P. Villano, M. Berrettoni, S. Passerini, *J. Electrochem. Soc.* **148**, A1171–A1178 (2001)
45. V.M. Mohan, V. Raja, P.B. Bhargav, A.K. Sharma, V.V.R.N. Rao, *J. Polym. Res.* **14**, 283–290 (2007)
46. C. Shiun Liao, W. Bin Ye, *J. Polym. Res.* **10**, 241–246 (2003)
47. S. Mitra, A.R. Kulkarni, *Solid State Ionics* **154**, 37–43 (2002)
48. S.M. Pawde, K. Deshmukh, *Polym. Eng. Sci.* **49**, 808–818 (2009)
49. A.R. Polu, R. Kumar, V. Causin, R. Neppalli, *J. Korean Phys. Soc.* **59**, 114–118 (2011)
50. G.B. Appetecchi, F. Croce, B. Scrosati, *J. Electrochim. Acta* **40**, 991–997 (1995)
51. G.B. Appetecchi, G. Dautzenberg, B. Scrosati, *J. Electrochem. Soc.* **143**, 6–12 (1996)
52. M.S. Jayswal, D.K. Kanchan, P. Sharma, M. Pant, *Solid State Ionics* **186**, 7–13 (2011)
53. S.G. Rathod, R.F. Bhajantari, V. Ravindrachary, P.K. Pujari, T. Sheela, *J. Adv. Dielectrics* **4**, 1450033–1450039 (2014)
54. M. Singh, V.K. Singh, K. Surana, B. Bhattacharya, P.K. Singh, H.W. Rhee, *J. Ind. Eng. Chem.* **19**, 819–822 (2013)
55. K.S. Kim, S.B. Lee, H. Lee, H.S. Kim, Y. Lee, K. Kwack, *J. Ind. Eng. Chem.* **15**, 657–660 (2009)
56. H.J. Woo, S.R. Majid, A.K. Arof, *Mater. Chem. Phys.* **134**, 755–761 (2012)
57. M.K. Mohanapriya, K. Deshmukh, M.B. Ahamed, K. Chidambaram, S.K.K. Pasha, *Int. J. Chem. Tech. Res.* **8**, 32–41 (2015)
58. K. Ramly, M.I.N. Isa, A.S.A. Khair, *Mater. Res. Innov.* **15**, S82–S85 (2011)
59. M.H. Buraidah, L.P. Teo, S.R. Majid, A.K. Arof, *Phys. B* **404**, 1373–1379 (2009)
60. J.R. Macdonald (ed.), *Impedance Spectroscopy—Emphasizing Solid Materials and Systems* (Wiley-Interscience, New York, 1987)
61. B. Tareev, *Physics of Dielectric Materials* (MIR Publications, Moscow, 1979)
62. L. Fan, Z. Dang, G. Wei, C.W. Nan, M. Li, *Mater. Sci. Eng., B* **99**, 340–343 (2003)
63. A.R. Polu, H.W. Rhee, *Adv. Polym. Tech.* (2015). doi:[10.1002/adv.21581](https://doi.org/10.1002/adv.21581)
64. M.K. Mohanapriya, K. Deshmukh, M.B. Ahamed, K. Chidambaram, S.K.K. Pasha, *Mater. Today Proceed.* **3**, 1864–1873 (2016)